

SEPTEMBER 2011

RubberWorld

THE TECHNICAL SERVICE MAGAZINE FOR THE RUBBER INDUSTRY VOLUME 244, No. 6

**Advances in structure
measurements of carbon black**



Carbon black intra-aggregate void volume from dynamic compression measurements

by George A. Joyce and William M. Henry, *Columbian Chemicals*, and Anthony W. Thornton and John C. Hodgins, *Micromeritics Instrument*

Carbon blacks are characterized by their aciniform morphology or grape-like structure comprised of particles fused together as rigid structures termed aggregates. Within a given mass of product there exists a distribution of aggregate size and shape commonly referred to as structure. A more precise definition of carbon black structure from a rubber technologist's perspective is the total intra-aggregate void volume per unit mass. Structure plays an important role in many processing and performance properties of filled compounds.

Quality measurements of carbon black structure devised nearly half a century ago using dibutyl phthalate oil absorption do not always discriminate this important feature of carbon black, which is known to exhibit a dependency with the bulk density of a carbon black. Another important consideration for structure measurement is the state of aggregate reduction in a filled compound. In the major applications of carbon black, the filler or pigment exists in a dispersed state within a polymeric system, with some degree of aggregate reduction occurring during the dispersion process. These issues along with recent environmental concerns with phthalates have accelerated the need to develop an improved quality test to replace oil absorption. Studies within this laboratory in 2005 (ref. 1) demonstrated that compressed void volume is an improved structure measurement.

Recent advances with instrumentation include the development of scan-rate or stress controlled compression analyzers that are designed to measure carbon black structure from a single uniaxial compression. These modern analyzers have demonstrated rapid and repeatable compressibility data with applied pressure. Independent research groups have demonstrated these new instruments provide an improved measure of structure compared to oil absorption methods (refs. 2 and 3). These studies included assessments of SBR and NR compound properties including processability and reinforcement.

This article focuses on the known complications associated with uniaxial compression of powders in a cylinder due to sample-wall friction, and presents an instrument configuration and analysis technique that isolates effects of wall friction. The proposed method of void volume measurement represents an intrinsic material characteristic of carbon black, i.e., intra-aggregate void volume.

Calculations

Calculation of measured void volume, VV_M , is shown in equation 1 (ref. 4):

$$VV_m = \left(\frac{V_a - V_t}{m} \right) 100 \quad (1)$$

where V_a is equal to the apparent volume of the sample in cm^3 ,

V_t is equal to the theoretical volume of the solid sample in cm^3 , and m is the sample mass in grams. The unit of measure for VV_M is $\text{cm}^3/100\text{g}$. The apparent volume, V_a , is defined by equation 2:

$$V_a = \frac{h \times \pi D^2}{4} \quad (2)$$

where h equals the measured sample height in cm, and D is equal to the cylinder diameter in cm. The theoretical solid sample volume, V_t , is defined by equation 3:

$$V_t = \frac{m}{\rho_t} \quad (3)$$

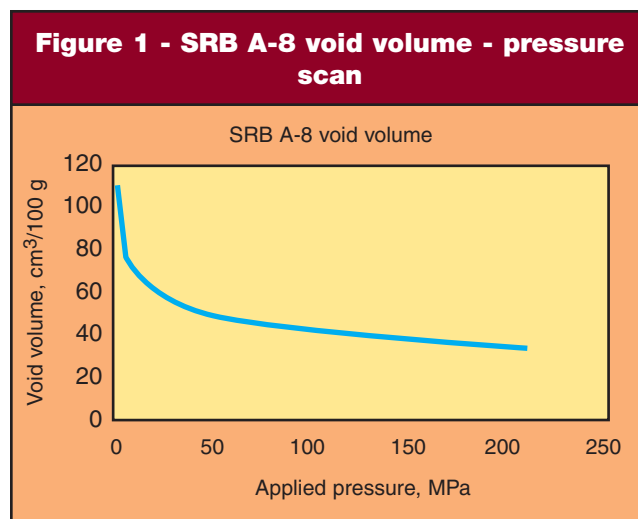
where m is the sample mass in grams and ρ_t is the true or skeletal density of carbon black (commonly accepted as 1.9 g per cm^3 for many carbon blacks) (ref. 5).

The measured sample height h at an applied pressure is determined by the axial position of the piston tip, z . Calibration of the piston tip displacement is typically achieved by measuring at least two axial reference positions, a zero height reference at the bottom of the cylinder, and one or more reference positions based on the height of steel calibration plugs.

A dynamic void volume analyzer from Micromeritics Corporation, DVVA4000 previously described (ref. 2), was used for all applied pressure experiments. Initial studies of sample mass with a cylinder of 12.70 mm (0.5 inch) diameter and scan rate of 69 MPa/min. led to several observations fundamental to compression of powder in a cylinder.

Applied pressure experiments

A representative void volume pressure scan of a tread grade carbon black is found in figure 1. The carbon black, ASTM SRB A-8, is an N326 and is characterized by a low structure level based on oil absorption number (OAN). This void volume scan from a single compression with 1 gram of sample mass was obtained over the applied pressure range of



1-210 MPa.

Carbon black void volume compression curves contain two characteristic regions. The first region is associated with a very rapid decrease in measured void volume due to sample de-aeration. This rapid decrease in apparent volume at low applied pressures is an attribute of the very fragile nature of carbon black agglomerations. At low pressure levels, a rapid consolidation and compaction of the carbon black takes place with a corresponding increase in apparent density.

The second region of the compression curve is associated with very small changes in void volume and corresponding large changes in applied pressure. This region of the pressure scan is associated with close packing of the carbon black aggregates and agglomerates, typically found at applied pressures greater than 30-50 MPa. From this point in the pressure scan, the application of additional pressure results in only small changes in apparent volume due to minor sample consolidation and deformation along with some breakage of weaker aggregate branches (ref. 6). In this region of the pressure scan, where inter-aggregate void space has been minimized and some aggregate reduction has taken place, com-

pressed void volumes have been shown to exhibit optimum relationships to compound processability and reinforcement properties (ref. 2).

Plots of the SRB A-8 at sample masses of 1-3 grams are shown in figure 2. These three pressure scans do not overlay each other and demonstrate a dependency of the void volume measure with sample mass, a complication related to the sample-wall friction and non-homogenous density distribution due to compaction in a cylinder. In the absence of wall friction, each of the scans in figure 2 would be equivalent, regardless of sample mass, as implied by equation 1. Sample mass dependency is a known complication with uniaxial compression measurements.

Void volume scans for the SRB A-8 at different masses were analyzed at constant pressures to further demonstrate mass dependence. The SRB A-8 void volumes at 50 and 100 MPa applied pressures were plotted with sample mass, shown in figure 3. In figure 3, a linear dependence of the void volume with sample mass is demonstrated for each of the applied pressures. The intercept of these linear lines provides an estimation of the void volume at an infinitely small sample mass that should have an aspect ratio free of the effects of wall friction.

Studies of pharmaceutical and other powders (refs. 7-9) have identified force losses due to sample-wall friction by demonstrating that transmitted forces through a sample are less than the force applied to a sample. The level of applied pressure, die wall friction coefficient and aspect ratio are some of the key parameters in describing radial force losses. These studies further demonstrated that friction coefficients are not constant, but vary with applied pressure and apparent density of the compact.

An estimate of friction coefficients, α , for carbon black compression in a 12.70 mm (0.5 inch) diameter cylinder was calculated using the slope of linear regressions of void volume mass plots at each increment of applied pressure. Estimates for each of the ASTM SRB-8 series, shown in figure 4, demonstrate these friction estimates vary by carbon black grade, ap-

Figure 2 - SRB A-8 void volume and sample mass

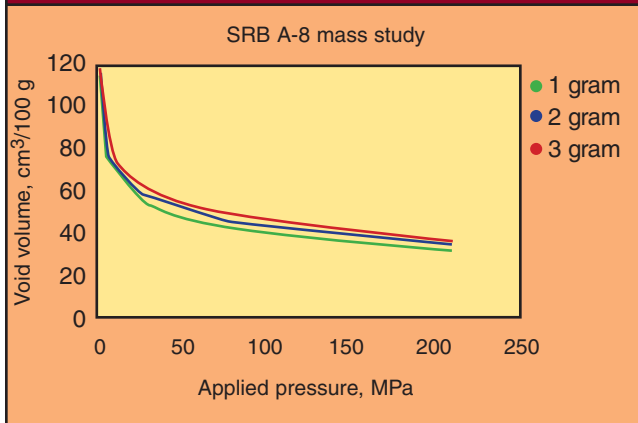


Figure 3 - SRB A-8 void volume and sample mass at 50 and 100 MPa P_a

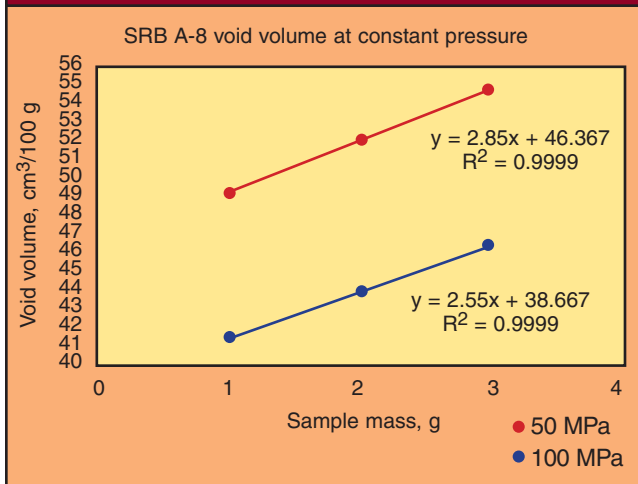
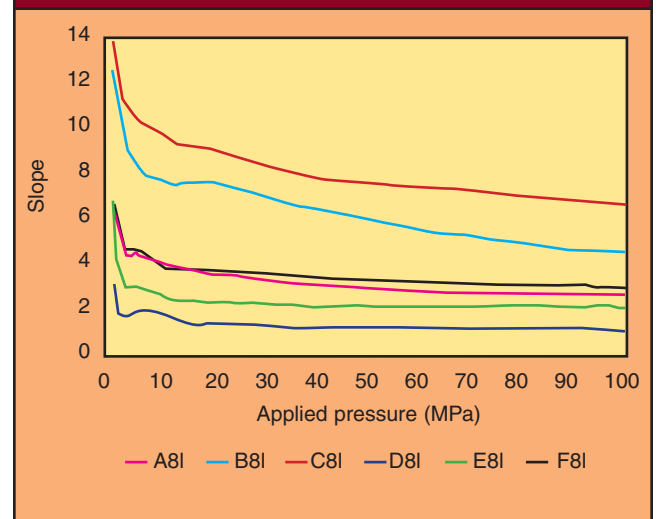


Figure 4 - estimates of wall friction for SRB-8 series



plied pressure and apparent density. These estimates are also ordered from highest to lowest structure. Even if normalized for carbon black structure level, these friction coefficients are not constant, but vary with applied pressure and apparent density. This observation indicates a constant friction coefficient cannot be used to properly correct applied pressure scans.

Additional pressure scans were collected on a high structure carbon black SRB C-7 at 20 MPa applied pressure, using cylinders of increasing diameter to observe effects of wall friction at different aspect ratios. Compression experiments in figure 5 included void volume measurements with three cylinder diameters of 12.70, 15.88 and 40.16 mm and mass levels of one to ten grams.

The dependency of void volume with sample mass is observed to be strongly influenced by cylinder diameter, as indicated in figure 5. The smallest cylinder diameter was 12.70 mm (0.5 inch) and exhibits the largest slope. The largest cylinder diameter of 40.16 mm (1.58 inch) exhibits the smallest slope or dependence on sample mass. The regression lines for the void volume-mass data for each cylinder exhibit a common intercept of approximately 97 cm³/100g, the only void volume measure common to each of the three cylinders. These experiments indicate that the lowest aspect ratios or height to diameter (h/D) exhibit the smallest friction coefficient estimates. However, even a very low aspect ratio will not produce void volume-applied pressure data free of wall friction effects, and requires correction using an appropriate methodology.

Multi-load cell compression analysis

Uniaxial compression of pharmaceutical powders for tableting has been studied for many years using presses configured with two or three load cells used to measure applied, transmitted and frictional forces. Triaxial compression testing is a common technique for characterizing the strength and stress-strain properties of soils and building materials. Powder technology describing both experimental and numerical analysis of powder compression is well developed (refs. 10-14). Recently, a new prototype void volume analyzer was developed by Micromeritics Corporation to enable a more detailed analysis of

Table 1 - compact aspect ratios and estimates for SRB C-7

Cylinder Dia., mm	VV at 20 MPa cm ³ /100 g	h/D	α estimates
12.70	105.8	0.9850	8.9
15.88	101.3	0.4896	3.75
40.16	100.1	0.2954	0.274

compression data. This prototype analyzer was configured with an instrumented cylinder to measure applied forces, transmitted forces through the sample, and radial force loss due to friction. A diagram of the instrumented cylinder is shown in figure 6.

The prototype DVVA was initially configured with a 12.70 mm diameter cylinder (0.5 inch). Analysis of force signals from the initial compression experiments at 23°C provided insightful information regarding force losses due to friction.

Compression forces for an N326 tread type carbon black, ASTM SRB A-8, are shown in figure 7. This scan includes

Figure 6 - instrumented cylinder

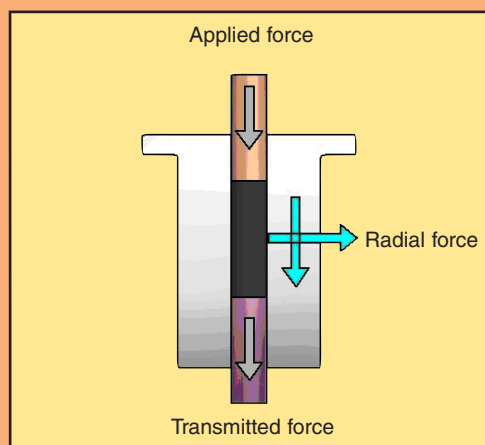


Figure 5 - effect of aspect ratio and sample mass on SRB C-7 void volume

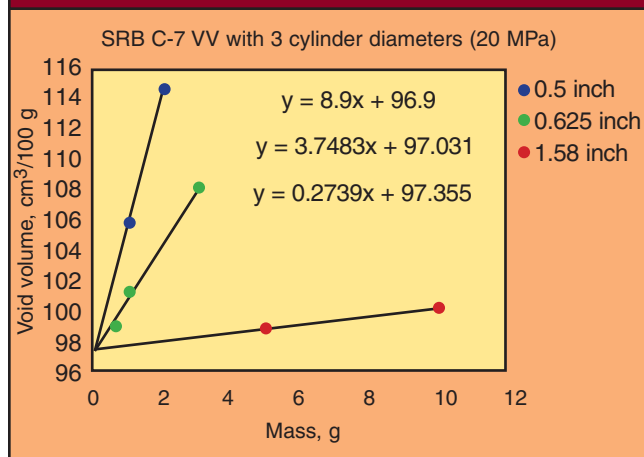
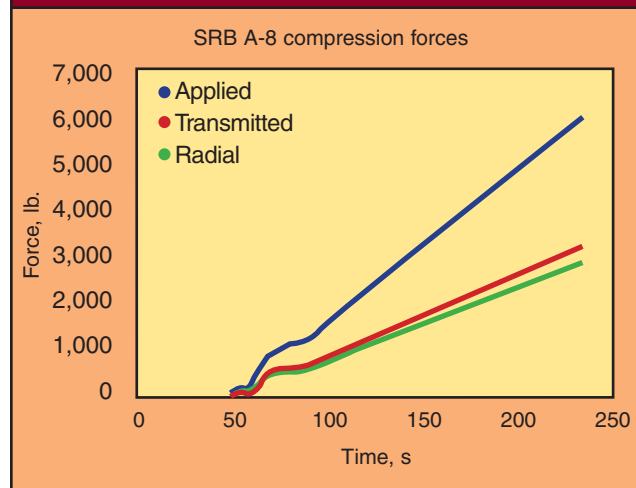


Figure 7 - compression forces for 1 g of SRB A-8



measured forces from each of the three load cells per unit time, including applied force, transmitted force and radial force. Based on this scan data and many other compression experiments of carbon blacks, the applied force was observed to be equivalent to the sum of the transmitted and radial forces, within error of the measurements. Therefore, the transmission force is equal to the difference in applied and radial forces, as defined in equation 4.

$$F_t = F_a - F_r \quad (4)$$

Figure 7 provides experimental evidence that the difference in the applied force and the force transmitted through a sample is equivalent to the radial force loss.

Tabular data from the scans shown in figure 7 are summarized in table 2. For a given time interval, the sum of the transmitted and radial forces is observed to be equivalent to the applied force, within measurement error of the force transducers.

Other information describing compaction behavior is the ratio of radial to axial stress, or transfer ratio. Within this constant rate scan, the transfer ratio was observed to be constant at 0.47, similar to values reported for other powders found in the literature.

Force transmission through a carbon black sample

In a single uniaxial compression, the relationship between the applied force, F_a , and the transmitted force, F_t , is often expressed exponentially as defined in equation 5,

$$F_t = F_a * e^{-kh/D} \quad (5)$$

where k is a material dependent constant for wall friction and h and D are height and diameter of the compact. Based on equation 5 and the experimentally derived data previously discussed, estimated friction coefficients are not constants for a given aspect ratio or applied pressure, and vary with carbon black structure level. In the absence of a constant friction coefficient and aspect ratio, the transmitted force through a sample

Table 2 - force signals from compression scan of SRB A-8

Time s	Applied force lb.-force	Transmitted force lb.-force	Radial force lb.-force	Transmitted + radial forces	Transfer ratio
74.9	991	519	468	987	0.47
100.2	1,562	826	732	1,558	0.47
150.2	3,198	1,679	1,509	3,188	0.47
199.9	4,830	2,536	2,276	4,812	0.47

bed cannot be calculated; therefore, measurement of the transmitted force is required to properly characterize powder compression.

Void volume pressure scans shown in figure 8 demonstrate the loss of transmitted pressure through a carbon black sample.

Figure 8 includes three void volume scans representing applied (dash) and transmitted (dot) pressures for an N660 carbon black (ASTM SRB E-8) at sample masses of 1 (blue), 2 (red) and 3 (green) grams in a 12.70 mm (0.5 inch) cylinder. These scans demonstrate the effect of radial force loss in the pressure measurements based on applied and transmitted pressures, and the effect of varying sample mass. This information underscores the need for appropriate pressure corrections.

Force averaging

In an instrumented cylinder, as previously described, the conservation of applied force is observed experimentally. There exists a balance of axial forces such that the applied force at the upper piston tip is equal to the sum of the force transmitted through the sample plus the radial force loss due to friction at the sample-wall interface:

$$F_a = F_t + F_r \quad (6)$$

Y. Tien, et al, and Patel (refs. 15 and 16) describe the use of a mean compaction force, F_M , as a practical friction-independent measure of compaction load which is not possible from the use of only applied force or transmitted force measurements:

$$F_m = (F_a + F_t) / 2 \quad (7)$$

Several methods of averaging axial forces or pressures have been reported, including arithmetic, integral and geometric mean. These are found in equations 8-10.

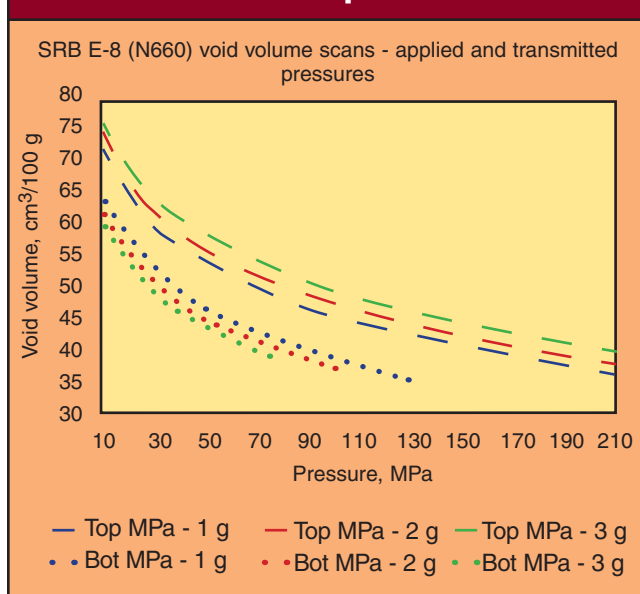
$$\text{Arithmetic mean } P_M = \frac{P_a + P_t}{2} \quad (8)$$

$$\text{Integral mean } P_{IM} = \frac{P_t - P_a}{\ln\left(\frac{P_t}{P_a}\right)} \quad (9)$$

$$\text{Geometric mean } P_{GM} = (P_a \times P_t)^{0.5} \quad (10)$$

Each of these mean pressures was evaluated to experimentally determine which offered the best approximation of central tendency or independence of sample mass and cylinder geometry with carbon blacks. Void volume pressure scans shown in figures 9 and 10 include arithmetic (blue), integral (green) and geometric (red) mean pressure scans. The carbon black analyzed in figure 9 is an N326 low structure tread type (ASTM SRB A-8). The carbon black in figure

Figure 8 - N660 void volume at applied and transmitted pressures



10 is a very high structure N100 type (ASTM SRB C-8).

In a cylinder where the applied force transmission decays exponentially, a geometric mean pressure, PG_M , should provide the best approximation of the central tendency. In both of the assessments of the three mean pressures shown in figures 9 and 10, and other assessments not included in this paper, the geometric mean pressure consistently exhibited the tightest grouping of scans.

The independence of both sample mass and aspect ratio was examined with geometric mean pressure averaging and is shown in figure 11. In this series of void volume pressure scans, the SRB F-8 (N683) was compared in two cylinders of 12.70 and 15.88 mm diameter (0.5 and 0.625 inch) and sample masses of 1 to 4.7 g. Figure 11 includes a total of 15 different scans overlaid on each other. Based on the consistent scan profiles, this series of experiments confirms the independence of void volume with sample mass and aspect ratio when using a geometric mean pressure average.

A similar series of experiments was made in which both

sample mass and aspect ratio were examined with geometric mean pressure averaging, and then further analyzed by interpolating data using both measurement signals (height and force). In typical experiments of geometric mean pressure averaging, the applied and transmitted pressure data are averaged based on interpolating them to common units of void volume. In this series of experiments, scan data were also interpolated to common units of pressure and the corresponding void volumes averaged using a geometric mean.

Figure 12 includes twelve scans with the SRB E-8 (N660) which are overlaid. These scans include six different sample masses and two different cylinder diameters, and interpolation by the two techniques described above. The results shown in figure 12 indicate that both methods of interpolation produce equivalent scan profiles when averaged with a geometric mean. This series of experiments again confirms the independence of void volume with sample mass and aspect ratio when using a geometric mean pressure average.

The consistency of void volume-pressure scans using different cylinder diameters, sample masses and various carbon blacks offers sufficient experimental evidence demonstrating that geometric mean pressure averaging provides a true void volume pressure scan that represents material characteristics of the carbon black sample (i.e., total intra-aggregate void volume).

ASTM SRB series-8 void volume at geometric mean pressure

A Micromeritics DVVA instrumented with dual load cells to measure applied and transmitted force was utilized to collect void volume-pressure scans for the ASTM SRB-8 series carbon blacks. These six reference carbon blacks represent tread and carcass types, products which are utilized in tires and other applications.

Scans were collected from 1-210 MPa applied pressure at 69 MPa/min. at three different sample masses in a 12.70 mm diameter cylinder (0.5 inch). Scans for each of the six reference carbon blacks are shown in figures 13-18. Each figure includes overlays of applied, transmitted and geometric mean pressures for each of the three sample masses.

For each of the six ASTM standard reference blacks, void volume scans at geometric mean pressures are essentially constant for the three different sample masses. This information further demonstrates that the geometric mean pressure correction isolates the effects of radial force loss due to sample-wall friction.

Tabular data from each of the one gram scans shown in figures 13-18 are summarized in table 3. The void volume at geomet-

Figure 9 - N326 void volume at mean pressures including numerical, integral and geometric

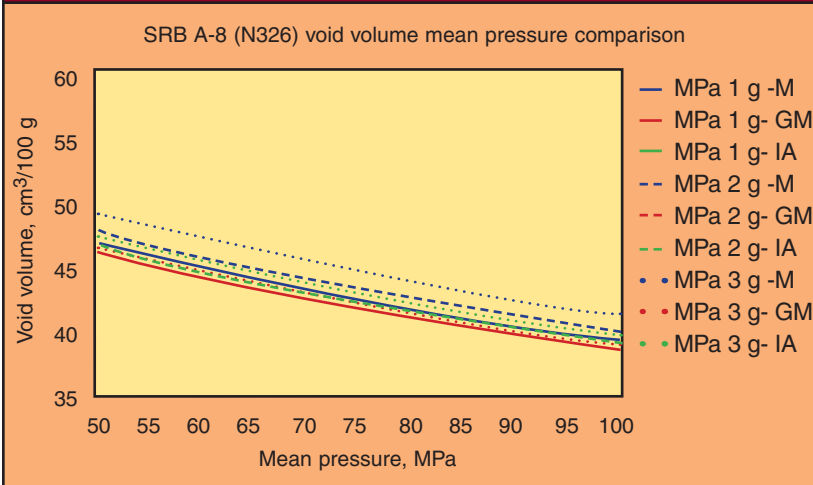
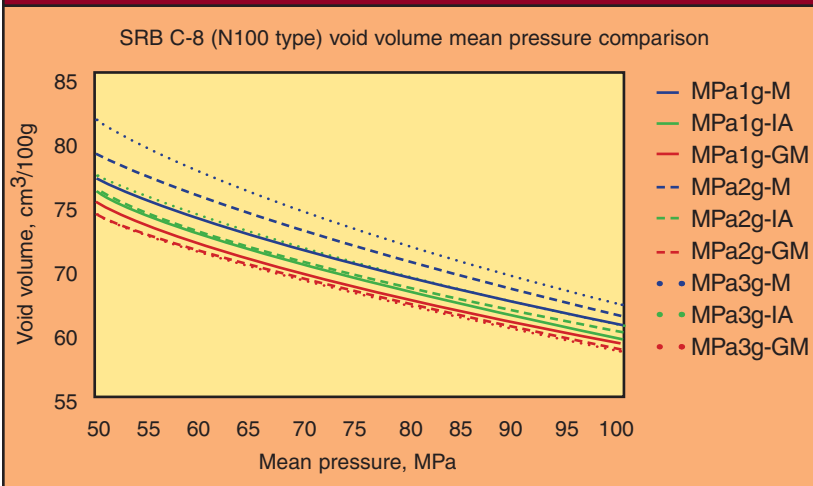


Figure 10 - SRB C-8 void volume at mean pressures including numerical, integral and geometric



ric mean pressures of 50 - 100 MPa are presented for use as a single parameter quality measurement to eventually replace oil absorption methods as the primary measure of carbon black structure.

Conclusions

Carbon black void volume measurements obtained from dynamic compression analyzers have been studied as a result of known complications with uniaxial compression of powder due to sample-wall friction. Several configurations of instrumented cylinders have been studied along with the use of pressure averaging methods. Void volume scans at geometric

Table 3 - SRB-8 structure measurements

ASTM SRB-8	Grade	OAN * cm ³ /100 g	COAN * cm ³ /100 g	VV 50 MPa (P _{GM}) cm ³ /100 g	VV 75 MPa (P _{GM}) cm ³ /100 g	VV 100 MPa (P _{GM}) cm ³ /100 g
A-8	N326	71.0	66.6	45.2	40.8	37.7
B-8	N134	123.8	99.8	69.4	61.5	56.0
C-8	HS N100	174.7	130.8	73.1	63.8	57.3
D-8	LS N700	38.9	38.6	23.9	22.1	20.8
E-8	N660	87.7	74.9	49.5	44.7	41.3
F-8	N683	131.8	88.6	60.3	53.0	48.1

* ASTM target values

mean pressures have been found to provide compression data isolated from the effects of sample-wall friction. Dynamic compression analyzers configured with two load cells measuring applied and transmitted forces can generate void volume-pressure scans which are independent of both sample mass and cylinder diameter. This improved structure measurement now represents an intrinsic material characteristic of carbon black directly related to intra-aggregate void volume.

Dynamic compression analyzers configured with two load cells measuring applied and transmitted forces can generate void volume-pressure scans which are independent of both sample mass and cylinder diameter. This improved structure measurement now represents an intrinsic material characteristic of carbon black directly related to intra-aggregate void volume.

References

1. G.A. Joyce and W.M. Henry, "Modeling the equilibrium void volume of carbon black," *Rubber Chem. And Technol.* 79, 735 (2006).
2. G.A. Joyce, W.M. Henry and R. W. Magee, "Advances in structure measurements of carbon black," *Rubber World* 240 (6), 27 (2009).
3. Y. Leiner, D. Roller and J. Lacayo-Pineda, "Compressed volume structure test," presented to ASTM D24.11 Subcommittee Meeting, June 8, 2010.
4. ASTM Standard D6086-09a, 2009, ASTM International, West Conshohocken, PA.
5. ASTM Standard D6556-09, 2009, ASTM International, West Conshohocken, PA.
6. A. Medalia and R.L. Sawyer, "Proceedings of the fifth conference on carbons," 563 (1961).
7. A. Michrafy, J.A. Dodds and M.S. Kadiri, "Wall friction in the compaction of pharmaceutical powders: Measurement and effect on the density distribution," *Powder Technol.* 148 (2004) 53-55.
8. B.J. Briscoe and S.L. Rough, "The effects of wall friction in

Figure 11 - N683 void volume at geometric mean pressures with varying mass and cylinder diameter

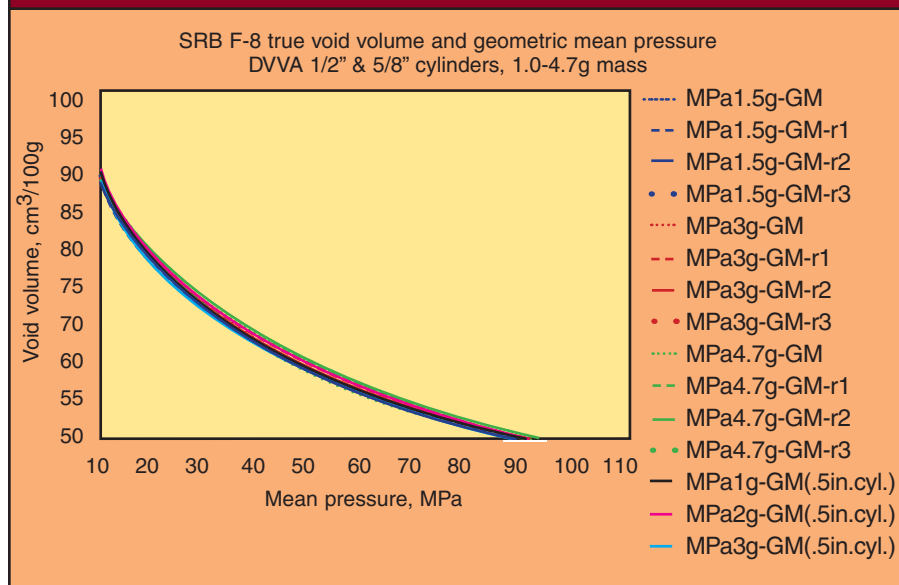
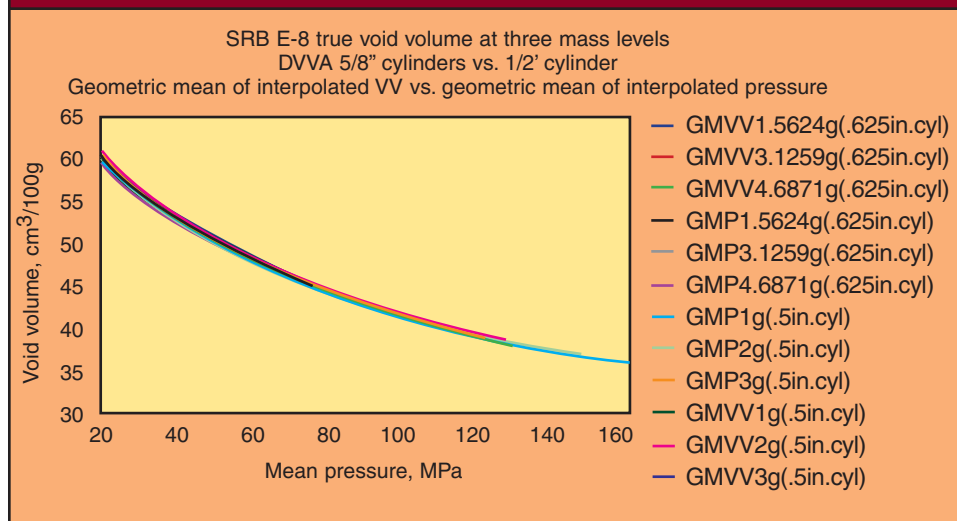


Figure 12 - N660 void volume at geometric mean pressure with varying mass, cylinder diameter and interpolation method



powder compaction," *Colloids Surf., A Physicochem. Eng. Asp.* 137 (1998) 103-116.

9. J.C. Cunningham, I.C. Sinka and A. Zavaliangos, "Analysis of tablet compaction 1. Characterization of mechanical behavior of powder/powder tooling friction," *J. Pharm.* 93 (2004) 2,022-2,039.

10. M.S. Kadiri, A. Michrafy and J.A. Dodds, "Pharmaceutical powders compaction: Experimental and numerical analysis of the density distribution," *Powder Tech.*, 157 (2005) 176-182.

11. R.M. Nedderman, *Statics and Kinematics of Granular*

Materials, Cambridge University Press, 1992.

12. M.S. Nielsen, N. Bay, M. Eriksen, J.I. Bech and M.H. Hancock, "An alternative to the conventional triaxial compression test," *Powder Technol.* 161 (2006) 220-226.

13. Y.M. Tien, P.L. We, W.H. Juang, M.F. Kuo and C.A. Chu, "Wall friction measurement and compaction characteristics of bentonite powders," *Powder Technol.* 173 (2007) 140-151.

14. C.Y. Wu, O.M. Ruddy, A.C. Bentham, B.C. Hancock, S. M. Best and J.A. Elliott, "Modeling the mechanical behavior of pharmaceutical powders during compaction," *Powder Technol.* 152 (2005) 107-117.

Figure 13 - SRB A-8 void volume applied, transmitted and geometric mean pressures

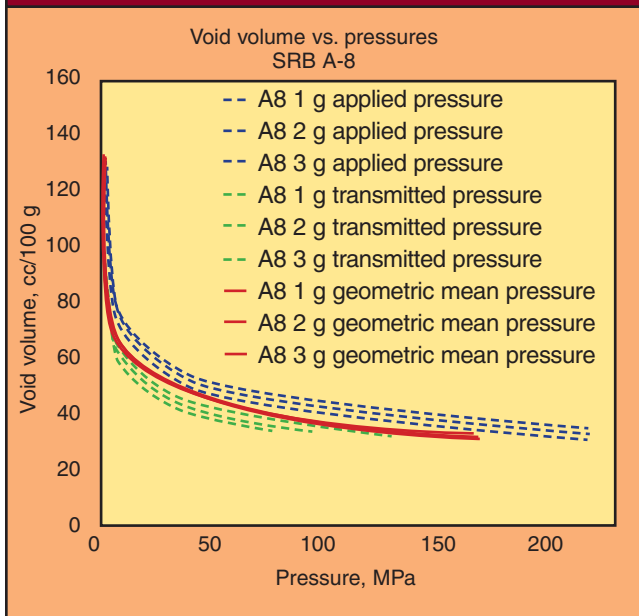


Figure 15 - SRB C-8 void volume applied, transmitted and geometric mean pressures

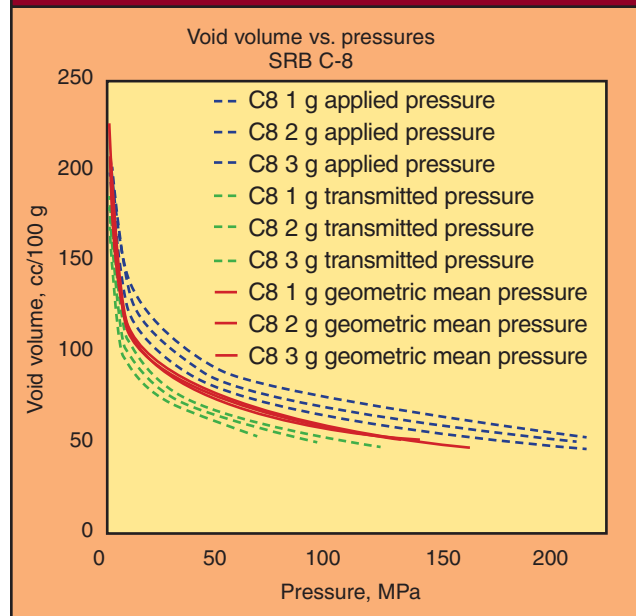


Figure 14 - SRB B-8 void volume applied, transmitted and geometric mean pressures

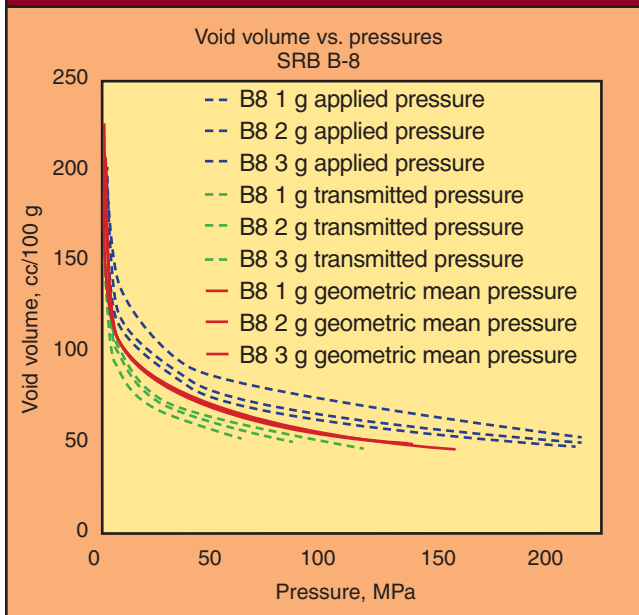


Figure 16 - SRB D-8 void volume applied, transmitted and geometric mean pressures

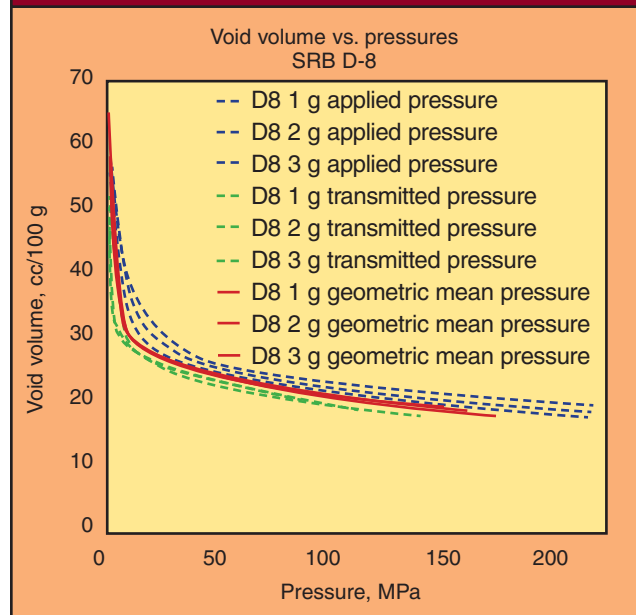


Figure 17 - SRB E-8 void volume applied, transmitted and geometric mean pressures

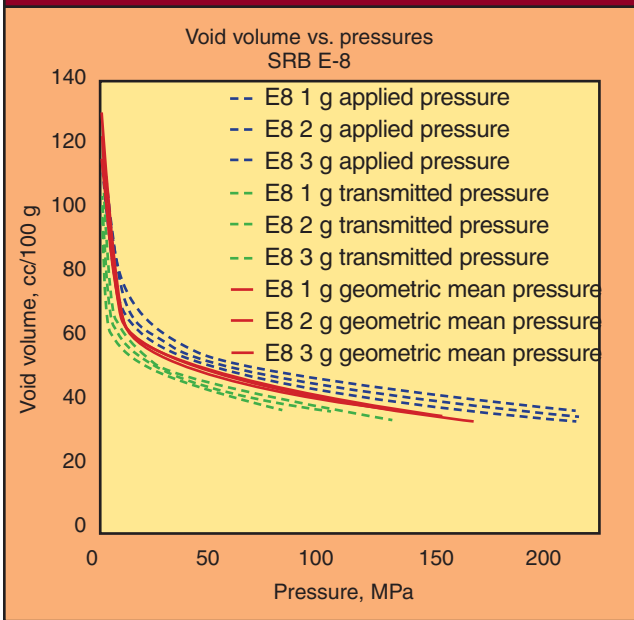
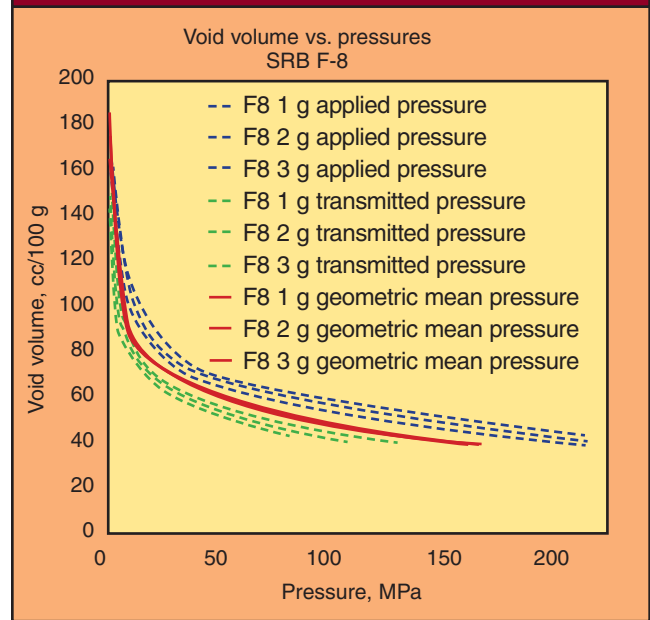
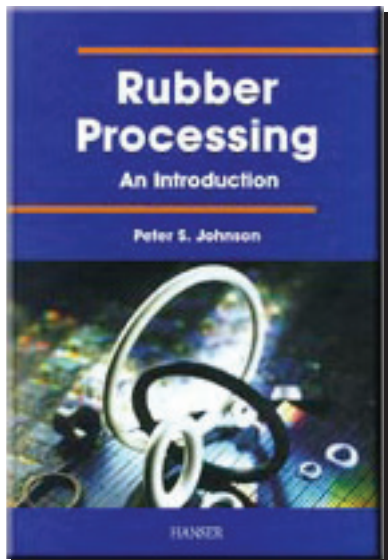


Figure 18 - SRB F-8 void volume applied, transmitted and geometric mean pressures



15. Y.M. Tien, P.L. Wu, C.A. Chu, W.S. Chuang and L.H. Wu, "The friction-free compressibility curve of bentonite block," *Physics and Chem. of the Earth* 32 (2007) 809-819.

16. Patel & Patel, "Overview of phenomenological equations for powder compaction study," *Int. J. Pharmaceutical Res.* (2009) 1 (1) 2-15.



ISBN 1-56990-309-3
2001, 141 pages
44 figures, Hardcover
\$70.00

Call: 330-864-2122 to order
or visit www.rubberworld.com

Rubber Processing:

An Introduction

By Peter S. Johnson

Addresses all aspects of rubber processing: mixing, milling, calendering, extrusion, and molding, and also testing and specification of raw materials, mixed compounds, and end products. It also covers the importance of flow behavior (rheology) in rubber processing and combines basic theory with its application in practice.

Rubber Processing is for both newcomers to the rubber industry, who want an overview of rubber processing and for those, who have regular involvement with some aspect of rubber processing, whether as suppliers to the industry, as processors, or as end-product users.

CONTENTS:

- Chapter 1** - Overview of Rubber Processing.
- Chapter 2** - Raw Materials Acceptance and Specification.
- Chapter 3** - Mixing of Rubber Compounds.
- Chapter 4** - Flow Behavior of Compounds.
- Chapter 5** - Testing of Compound after Mixing.
- Chapter 6** - Curing Process.
- Chapter 7** - Calendering of Rubber.
- Chapter 8** - Extrusion of Rubber.
- Chapter 9** - Molding of Rubber.
- Chapter 10** - Finished Product Testing.

"Dr. Johnson has provided the most thoroughgoing review of all the aspects of conventional rubber processing that has come along in decades." --review by R.J. Del Vecchio, Technical Consulting Services

Carbon Blacks for Rubber

Dimensional Classification
of Carbon Blacks for the
Rubber Industry

Columbian TM
Corporate Headquarters
1800 West Oak Commons Court
Marietta, GA 30062
USA